

Articles

Conformational Study of 2,3,5,7,8,12,13,15,17,18-Decaalkylporphyrins

Craig J. Medforth,^{*,†} Mathias O. Senge,[†] Timothy P. Forsyth,[†] J. David Hobbs,[‡]
John A. Shelnutt,^{*,‡} and Kevin M. Smith^{*,†}

Department of Chemistry, University of California, Davis, California 95616, and Fuel Science
Department 6211, Sandia National Laboratories, Albuquerque, New Mexico 87185

Received January 6, 1994*

X-ray crystal structures are reported for two sterically crowded porphyrins: 3,5,7,13,15,17-hexaethyl-2,8,12,18-tetramethylporphyrin (**6**, H₂DAP) and (3,5,7,13,15,17-hexaethyl-2,8,12,18-tetramethylporphyrinato)nickel(II) (Ni**6**, NiDAP). In the NiDAP structure, steric crowding is relieved by the usual mechanism of the porphyrin adopting a nonplanar conformation. The crystal structure of H₂DAP is unusual, as it shows an essentially planar conformation of the porphyrin macrocycle. In this case, steric crowding of the meso and pyrrole ethyl groups is relieved by a novel elongation of the macrocycle along the 5,15 axis. A detailed study is made of the solution conformations of H₂DAP, NiDAP, and the corresponding zinc(II) complex (ZnDAP), using optical spectroscopy, variable-temperature proton NMR spectroscopy, and molecular mechanics calculations. It is suggested that the two species observed in low-temperature proton NMR studies of H₂DAP and ZnDAP correspond to cis and trans conformations of the methyl groups of the meso ethyls, and not the syn and anti structures proposed previously (Maruyama; et al. *J. Phys. Org. Chem.* **1988**, *1*, 63). Crystal data: H₂DAP (**6**), C₃₆H₄₆N₄, *M_r* = 534.8, monoclinic, *P*2₁/*c*, *a* = 6.458(4) Å, *b* = 16.58(2) Å, *c* = 13.778(7) Å, β = 99.78(4)°, *V* = 1,454(2) Å³, *Z* = 2, *D_x* = 1.222 Mg·m⁻³, λ(Mo Kα) = 0.710 73 Å, μ = 0.072 mm⁻¹, 130 K, *R* = 0.069 for 1769 reflections with *F* > 4.0σ(*F*); NiDAP (Ni**6**), C₃₆H₄₄N₄Ni, *M_r* = 591.5, monoclinic, *P*2₁/*c*, *a* = 14.350(8) Å, *b* = 16.043(6) Å, *c* = 15.049(6) Å, β = 117.12(3)°, *V* = 3,083(2) Å³, *Z* = 4, *D_x* = 1.274 Mg·m⁻³, λ(Mo Kα) = 0.710 73 Å, μ = 0.660 mm⁻¹, 130 K, *R* = 0.072 for 3717 reflections with *F* > 4.0σ(*F*).

Introduction

Nonplanar conformations of porphyrins and related macrocycles have long been a source of considerable interest.^{1–3} Recently, efforts in this area have been directed toward the preparation of extremely nonplanar porphyrins as models for the nonplanar conformational distortions that are found in biological systems.^{4–6} It is believed that these nonplanar distortions may be one mechanism for modulating the optical, redox, and other properties of tetrapyrroles.^{4–6} We recently prepared a series of dodecasubstituted porphyrins (e.g. **1**) which adopt extremely nonplanar conformations both in the crystalline state and in solution.^{7–14} These porphyrins have provided detailed information about the effects of nonplanarity on the porphyrin macrocycle.

The nonplanarity of dodecasubstituted porphyrins such as **1** is caused by steric crowding of the peripheral substituents. During our studies^{7–14} a systematic investigation was made of the factors that affect the degree of nonplanarity and the type of nonplanar distortion. It was found that the degree of nonplanarity could be modulated by the use of alkanoyl moieties fused to the pyrrole rings, with the degree of nonplanarity increasing dramatically in the series of porphyrins **2–4**.^{7,10,13} Changing the meso substituents to alkyl chains (as in e.g. **5**) was found to alter the type of nonplanar distortion and produced a ruffled porphyrin macrocycle.^{11,15} For the saddle-shaped porphyrin **1**, smaller metal ions such as nickel(II) were found to cause an increase in nonplanarity when compared to larger metals such as zinc(II).¹² The structural effects of various substituents and metal ions were accurately reproduced using a molecular mechanics force field designed specifically for porphyrins.^{10,12}

The above investigations prompted us to look at porphyrins which have fewer substituents than the dodecasubstituted porphyrins but which might still adopt nonplanar conformations. Such porphyrins are likely to provide further novel structural findings, as well as to provide a stringent test of the molecular mechanics force field and the spectroscopic techniques used to probe porphyrin nonplanarity. One porphyrin of interest is 3,5,7,-

[†] University of California.

[‡] Sandia National Laboratories.

* Abstract published in *Advance ACS Abstracts*, July 15, 1994.

- (1) Hoard, J. L. In *Porphyrins and Metalloporphyrins*; Smith, K. M., Ed.; Elsevier: Amsterdam, 1975; Chapter 8.
- (2) Scheidt, W. R. In *The Porphyrins*; Dolphin, D., Ed.; Academic Press: New York, 1979; Vol. 3, Chapter 10.
- (3) Scheidt, W. R.; Lee, Y. J. *Struct. Bonding* **1987**, *64*, 1.
- (4) Fajer, J.; Barkigia, K. M.; Smith, K. M.; Zhong, E.; Gudowska-Nowak, E.; Newton, M. In *Reaction Centers of Photosynthetic Bacteria*; Michel-Beyerle, M. E., Ed.; Springer-Verlag: Berlin, 1990; p 367.
- (5) Fajer, J. *Chem. Ind. (London)* **1991**, 869.
- (6) Senge, M. O. *J. Photochem. Photobiol., B* **1992**, *16*, 3.
- (7) Medforth, C. J.; Berber, M. D.; Smith, K. M.; Shelnutt, J. A. *Tetrahedron Lett.* **1990**, *31*, 3719.
- (8) Medforth, C. J.; Smith, K. M. *Tetrahedron Lett.* **1990**, *31*, 5583.
- (9) Barkigia, K. M.; Berber, M. D.; Fajer, J.; Medforth, C. J.; Renner, M. W.; Smith, K. M. *J. Am. Chem. Soc.* **1990**, *112*, 8851.
- (10) Shelnutt, J. A.; Medforth, C. J.; Berber, M. D.; Barkigia, K. M.; Smith, K. M. *J. Am. Chem. Soc.* **1991**, *113*, 4077.
- (11) Medforth, C. J.; Senge, M. O.; Smith, K. M.; Sparks, L. D.; Shelnutt, J. A. *J. Am. Chem. Soc.* **1992**, *114*, 9859.
- (12) Sparks, L. D.; Medforth, C. J.; Park, M.-S.; Chamberlain, J. R.; Ondrias, M. R.; Senge, M. O.; Smith, K. M.; Shelnutt, J. A. *J. Am. Chem. Soc.* **1993**, *115*, 581.

(13) Senge, M. O.; Medforth, C. J.; Sparks, L. D.; Smith, K. M.; Shelnutt, J. A. *Inorg. Chem.* **1993**, *32*, 1716.

(14) Barkigia, K. M.; Renner, M. W.; Furenlid, L. R.; Medforth, C. J.; Smith, K. M.; Fajer, J. *J. Am. Chem. Soc.* **1993**, *115*, 3627.

(15) The nomenclature used to describe nonplanar conformations is taken from ref 3. In a saddle conformation, alternate pyrrole rings are tilted up and down with respect to a least-squares plane through the 24 atoms of the porphyrin core and the meso carbon atoms are in the least-squares plane. In a ruffled conformation, alternate pyrrole rings are twisted clockwise or anticlockwise about the M–N bond such that the meso carbon atoms are alternately above or below the least-squares plane through the 24 atoms of the porphyrin core.

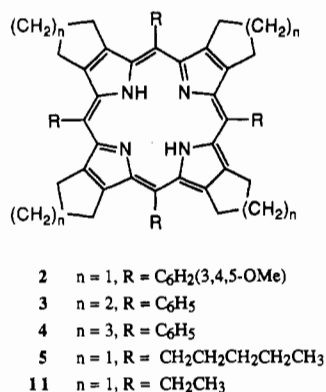
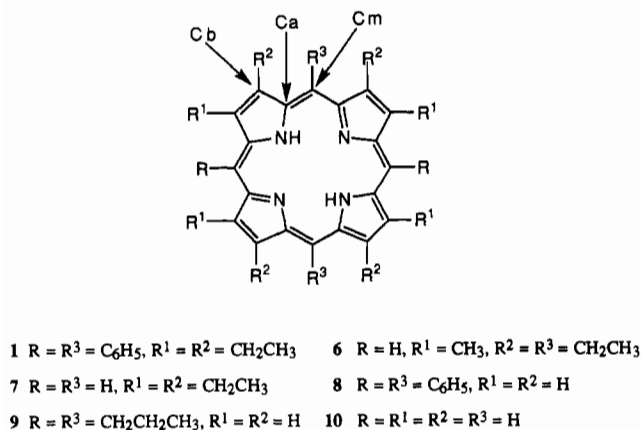


Figure 1. Structures and nomenclature for some deca-substituted and dodeca-substituted porphyrins. The conformations of the deca-substituted free-base porphyrin 6 and its metal complexes are investigated in this study.

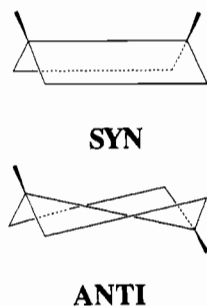


Figure 2. Solution structures previously proposed for H₂DAP and ZnDAP.¹⁶ Wedges indicate the substituents at the 5- and 15-positions. 13,15,17-hexaethyl-2,8,12,18-tetramethylporphyrin (6, H₂DAP). Variable-temperature proton NMR studies of H₂DAP and the corresponding zinc(II) complex (ZnDAP) have previously been interpreted in terms of a mixture of nonplanar syn and anti conformations (Figure 2).¹⁶ The copper(II) complex (CuDAP) has also been shown to adopt a syn structure in the crystalline state.¹⁷ In the present study, we report a comprehensive investigation of the conformations of H₂DAP, ZnDAP, CuDAP, and the nickel(II) complex (NiDAP), using X-ray crystallography, molecular mechanics calculations, optical spectroscopy, and variable-temperature proton NMR spectroscopy.

Experimental Section

Synthesis. H₂DAP was synthesized and purified using a literature procedure.¹⁶ To prepare NiDAP and ZnDAP, H₂DAP was dissolved in methylene chloride and a large excess of a saturated solution of either

Table 1. Crystal Data and Data Collection and Refinement Parameters for H₂DAP and NiDAP

	H ₂ DAP (6)	NiDAP (Ni6)
formula	C ₃₆ H ₄₆ N ₄	C ₃₆ H ₄₄ N ₄ Ni
habit	parallelepiped	hexagonal plate
mol wt	534.8	591.5
lattice	monoclinic	monoclinic
space group	P ₂ /c	P ₂ /c
a, Å	6.458(4)	14.350(8)
b, Å	16.58(2)	16.043(6)
c, Å	13.778(7)	15.049(6)
β, deg	99.78(4)	117.12(3)
V, Å ³	1,454(2)	3,083(2)
Z	2	4
D _{calcd} , g·cm ⁻³	1.222	1.274
μ, mm ⁻¹	0.072	0.660
λ(Mo Kα), Å	0.710 73	0.710 73
T, K	130	130
R ^a	0.069	0.066
R _w ^b	0.074	0.072
S	1.33	1.17

$$^a R = \sum |F_o| - |F_c| / \sum |F_o|, \quad ^b R_w = [\sum w(|F_o| - |F_c|)^2 / \sum w F_o^2]^{1/2}.$$

nickel(II) acetate or zinc(II) acetate in methanol was added. The mixture was refluxed until thin layer chromatography indicated the absence of starting material. The reaction mixture was then washed twice with water, and the organic layer was dried over anhydrous sodium sulfate and concentrated in vacuo. The resulting residue was purified by column chromatography using silica gel and petroleum ether/methylene chloride (4:1 v/v) as eluent. The appropriate fractions were concentrated in vacuo, and the resulting solid was recrystallized from methylene chloride/cyclohexane.

Spectroscopic Measurements. Proton NMR spectra were recorded in CD₂Cl₂ at a frequency of 300 MHz. All chemical shifts are given in ppm and have been converted to the δ scale using the CHDC₂ signal at δ 5.30. The variable-temperature unit was calibrated using a sample of methanol.¹⁸ Electronic absorption spectra were recorded on a Hewlett Packard 8450A spectrophotometer using methylene chloride as solvent.

X-ray Crystallography. Crystals were immersed in hydrocarbon oil, and a single crystal was selected, mounted on a glass fiber, and placed in a low-temperature N₂ stream.¹⁹ A Siemens R3m/V automatic diffractometer with a graphite-monochromator and a locally modified low-temperature device was used for data collection. Cell parameters were determined from 23 automatically centered reflections in the range 20° ≤ 2θ ≤ 30°. During the data collection, two standard reflections were measured every 198 reflections and showed only statistical variation (<2% change in intensity). The intensities were corrected for Lorentz and polarization effects, an absorption correction was applied using the program XABS,²⁰ and extinction effects were disregarded. All calculations were carried out on a Vax-station 3200. The H₂DAP structure was solved using direct methods, and the NiDAP structure was solved via a Patterson synthesis and subsequent expansion using the SHELXTL PLUS program system.²¹ Full-matrix least-squares refinement on |F|² was carried out using the same program system. All non-hydrogen atoms were refined with anisotropic thermal parameters. Hydrogen atoms were included at calculated positions using a riding model (C–H distance 0.96 Å, N–H distance 0.9 Å). Further details of the crystal data, structure solutions, and structure refinements for H₂DAP and NiDAP are listed in Table 1. Atomic coordinates and equivalent isotropic displacements for H₂DAP and NiDAP are given in Tables 2 and 3.

Molecular Mechanics Calculations. Molecular mechanics calculations using BIOGRAF software (Molecular Simulations, Inc.) were carried out and displayed on a Silicon Graphics 4D210 power series or 4D35 personal Iris workstation. The force field used in the calculations^{10,12} has been shown to accurately reproduce the crystal structures of both planar and nonplanar metalloporphyrins.^{10–12} The force constants were obtained

(16) Maruyama, K.; Nagata, T.; Osuka, A. *J. Phys. Org. Chem.* **1988**, *1*, 63.
 (17) Nagata, T.; Osuka, A.; Maruyama, K.; Toriumi, K. *Acta Crystallogr.* **1990**, *C46*, 1745.

(18) van Geet, A. L. *Anal. Chem.* **1970**, *42*, 679.
 (19) Hope, H. In *Experimental Organometallic Chemistry: A Practicum in Synthesis and Characterization*; Wayda, A. L., Darensbourg, M. Y., Eds.; ACS Symposium Series 357; American Chemical Society: Washington, DC, 1987; p 257.
 (20) Hope, H.; Moezzi, B. Program XABS. University of California, Davis, 1987.
 (21) Sheldrick, G. M. SHELXTL PLUS: Program for Crystal Structure Solution. Universität Göttingen, Germany, 1989.

Table 2. Atomic Coordinates ($\times 10^4$) and Equivalent Isotropic Displacement Coefficients ($\text{\AA}^2 \times 10^3$) for 3,5,7,13,15,17-Hexaethyl-2,8,12,18-tetramethylporphyrin (H_2DAP)

atom	x	y	z	$U(\text{eq})^a$
N(21)	4183(5)	6145(2)	4440(2)	20(1)
N(24)	2875(5)	4816(2)	6006(2)	19(1)
C(1)	2557(6)	6484(2)	4796(3)	20(1)
C(2)	2087(6)	7273(2)	4358(3)	21(1)
C(21)	416(6)	7821(2)	4623(3)	28(1)
C(3)	3415(6)	7403(2)	3719(3)	21(1)
C(31)	3361(6)	8174(2)	3119(3)	30(1)
C(32)	4652(7)	8856(2)	3663(3)	36(2)
C(4)	4776(6)	6678(2)	3777(2)	19(1)
C(5)	6457(6)	6510(2)	3255(3)	20(1)
C(51)	7030(6)	7140(2)	2548(3)	25(1)
C(52)	5946(7)	7013(2)	1486(3)	37(2)
C(16)	2409(6)	4218(2)	6640(3)	21(1)
C(17)	622(6)	4499(2)	7057(3)	21(1)
C(171)	-528(7)	4160(2)	7844(3)	27(1)
C(172)	-86(7)	4640(2)	8799(3)	35(1)
C(18)	32(6)	5227(2)	6626(3)	21(1)
C(181)	-1858(6)	5728(2)	6753(3)	27(1)
C(19)	1451(6)	5439(2)	5977(3)	19(1)
C(20)	1376(6)	6161(2)	5460(3)	20(1)

^a Equivalent isotropic U defined as one-third of the trace of the orthogonalized U_{ij} tensor.

from a normal-coordinate analysis for NiOEP²² and the DREIDING force field,^{23a} and equilibrium bond distances, bond angles, torsions, and inversions were adjusted to reproduce the crystal structure of triclinic B-NiOEP.²⁴ The parameters for zinc(II) and copper(II) are those described recently.¹² In the present work an exponential r^6 van der Waals function was used for the hydrogen atoms, and an electrostatic term was included in the calculations. Partial atomic charges were obtained using the charge equilibration method.^{23b} These modifications have been shown to improve the accuracy of the calculated conformational energies for metal complexes of dodecasubstituted porphyrins.^{25,26} Unfortunately, calculations could not be undertaken for H_2DAP because the appropriate force field parameters are not available. Use of the default parameters gives structures which are too nonplanar, as noted previously.¹¹

Results and Discussion

X-ray Crystallography. The crystal structure of H_2DAP is shown in Figure 3. Unusually for such a highly substituted porphyrin the macrocycle is basically planar. The mean deviation of the 24 porphyrin atoms from the least-squares plane of the nitrogen atoms is only 0.05 \AA , with half of the macrocycle being displaced slightly above and the other half slightly below the least-squares plane of the nitrogen atoms (Figure 4). There are no indications that the planar conformation of H_2DAP is the result of crystal packing forces, as the porphyrin planes are separated by 4.16 \AA and there is only a small degree of overlap between the porphyrin π systems. A striking feature of the structure of H_2DAP is an unusual elongation of the macrocycle along the 5,15 axis. This makes the macrocycle appear oblong rather than square (Figure 4). One measure of the elongation is the distance between N(21) and N(24) (3.29 \AA) versus that between N(21) and the other adjacent nitrogen N(24A) (2.63 \AA). As expected, the distances between opposite nitrogens are similar (N(21)–N(21A) = 4.17 \AA , N(24)–N(24A) = 4.26 \AA).

- (22) (a) Abe, M.; Kitagawa, T.; Kyogoku, Y. *J. Chem. Phys.* **1978**, *69*, 4526. (b) Li, X.-Y.; Czernuszewicz, R. S.; Kincaid, J. R.; Spiro, T. G. *J. Am. Chem. Soc.* **1989**, *111*, 7012. (c) Li, X.-Y.; Czernuszewicz, R. S.; Kincaid, J. R.; Stein, P.; Spiro, T. G. *J. Chem. Phys.* **1990**, *94*, 47.
- (23) (a) Mayo, S. L.; Olafson, B. D.; Goddard, W. A. *J. Phys. Chem.* **1990**, *94*, 88. (b) Rappé, A. K.; Goddard, W. A. *J. Phys. Chem.* **1991**, *95*, 3358.
- (24) Brennan, T. D.; Scheidt, W. R.; Shelnut, J. A. *J. Am. Chem. Soc.* **1988**, *110*, 3919.
- (25) Hobbs, J. D.; Majumder, S. A.; Luo, L.; Sickel-Smith, G. A.; Quirke, J. M. E.; Medforth, C. J.; Smith, K. M.; Shelnut, J. A. *J. Am. Chem. Soc.* **1994**, *116*, 3261.
- (26) Medforth, C. J.; Hobbs, J. D.; Rodriguez, M. R.; Abraham, R. J.; Smith, K. M.; Shelnut, J. A. *Inorg. Chem.*, in press.

Table 3. Atomic Coordinates ($\times 10^4$) and Equivalent Isotropic Displacement Coefficients ($\text{\AA}^2 \times 10^3$) for (3,5,7,13,1,17-Hexaethyl-2,8,12,18-tetramethylporphyrinato)nickel(II) (NiDAP)

atom	x	y	z	$U(\text{eq})^a$
Ni	2335(1)	1038(1)	4037(1)	18(1)
N(21)	2654(3)	1989(3)	4872(3)	20(2)
N(22)	3692(3)	1134(3)	4107(3)	20(2)
N(23)	2016(3)	81(3)	3208(3)	21(2)
N(24)	1004(3)	922(3)	4008(3)	18(2)
C(1)	2167(4)	2204(3)	5444(4)	24(2)
C(2)	2624(5)	2968(3)	5987(4)	27(2)
C(21)	2291(5)	3367(4)	6708(4)	40(3)
C(3)	3343(5)	3226(3)	5705(4)	28(2)
C(31)	4075(5)	3954(4)	6180(5)	40(3)
C(32)	3584(6)	4805(4)	5777(6)	57(4)
C(4)	3359(4)	2621(3)	4993(4)	24(2)
C(5)	4032(4)	2602(3)	4555(4)	24(2)
C(51)	4408(5)	3422(4)	4315(5)	37(3)
C(52)	3936(6)	3527(4)	3169(5)	47(3)
C(6)	4287(4)	1844(3)	4528(4)	23(2)
C(7)	5219(4)	1648(3)	4149(4)	25(2)
C(71)	6113(5)	2201(4)	4263(5)	37(3)
C(72)	6898(5)	2372(5)	5341(5)	49(3)
C(8)	5211(4)	814(3)	4008(4)	25(2)
C(81)	6006(5)	289(4)	3898(5)	34(3)
C(9)	4222(4)	508(3)	3916(4)	21(2)
C(10)	3788(5)	-255(3)	3498(4)	25(2)
C(11)	2737(5)	-424(3)	3101(4)	24(2)
C(12)	2211(5)	-1080(3)	2411(4)	30(3)
C(121)	2767(6)	-1757(4)	2140(5)	47(3)
C(13)	1163(5)	-953(3)	2035(4)	30(2)
C(131)	318(6)	-1559(4)	1386(5)	47(3)
C(132)	-128(6)	-2037(4)	2000(6)	57(4)
C(14)	1049(5)	-211(3)	2546(4)	25(2)
C(15)	116(5)	113(3)	2469(4)	26(2)
C(151)	-884(5)	61(4)	1479(4)	37(3)
C(152)	-755(6)	578(6)	700(5)	71(4)
C(16)	110(4)	554(3)	3260(4)	20(2)
C(17)	-743(4)	613(3)	3539(4)	25(2)
C(171)	-1812(5)	215(4)	3019(5)	32(3)
C(172)	-2683(5)	815(4)	2328(5)	47(3)
C(18)	-346(4)	1000(3)	4428(4)	26(2)
C(181)	-890(4)	1194(4)	5055(5)	36(3)
C(19)	717(4)	1236(3)	4687(4)	21(2)
C(20)	1297(4)	1815(3)	5409(4)	25(2)

^a Equivalent isotropic U defined as one-third of the trace of the orthogonalized U_{ij} tensor.

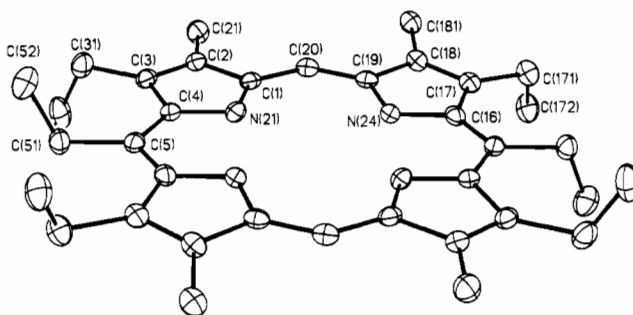


Figure 3. Molecular structure and numbering scheme for the crystal structure of H_2DAP . Ellipsoids are drawn for 50% occupancy; hydrogen atoms have been omitted for clarity.

The core size (defined as half of the average distance between opposite nitrogens) is 2.11 \AA , which is comparable to the core sizes seen in H_2OEP (7) (2.098 \AA), H_2TPP (8) (2.099 \AA), and H_2TPPr (9) (2.080 \AA).¹

The unusual elongation of the H_2DAP macrocycle was investigated by tabulating the bond lengths and bond angles according to whether they were associated with substituted or unsubstituted meso positions (Table 4). The differences in bond lengths between the substituted or unsubstituted meso positions are quite small, as are the differences in the bond angles of the pyrrole rings (N–Ca–Cb and Ca–Cb–Cb). In contrast, large differences between the substituted and unsubstituted meso

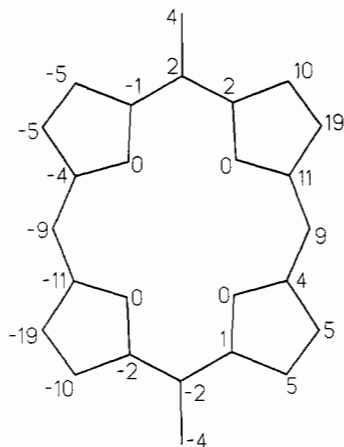


Figure 4. Deviations of atoms from the least-squares planes of the four nitrogen atoms in the crystal structure of H₂DAP ($\text{\AA} \times 10^2$).

Table 4. Average Out-of-Plane Displacements, Bond Lengths, and Bond Angles for H₂DAP and Other Free-Base Porphyrins

	H ₂ P (10)	H ₂ OEP (7)	H ₂ TPrP (9)	H ₂ DAP (6)	
				meso H	meso ethyl
Displacements (\AA) ^a					
N	0.01	0.05	0.03	0.00	
Ca	0.02	0.01	0.02	0.08	0.02
Cb	0.01	0.03	0.04	0.12	0.08
Cm	0.03	0.02	0.05	0.09	0.02
Bond Lengths (\AA) ^b					
N—Ca	1.377	1.366	1.374	1.367(5)	1.380(5)
Ca—Cb	1.442	1.450	1.440	1.440(5)	1.468(5)
Ca—Cm	1.382	1.392	1.397	1.392(6)	1.418(6)
Cb—Cb	1.355	1.363	1.347	1.359(6)	
Cb—CH _x				1.507(6)	1.521(6)
Cm—CH ₂				1.516(5)	
Bond Angles (deg) ^c					
N—Ca—Cm	125.3	125.1	126.8	128.7(4)	121.6(4)
N—Ca—Cb	108.9	109.3	108.1	108.6(3)	108.1(3)
Ca—N—Ca	107.4	107.7	108.3	108.5(3)	
Ca—Cm—Ca	127.1	127.6	125.0	133.8(4)	122.8(3)
Ca—Cb—Cb	107.5	106.9	107.8	108.5(3)	106.4(3)
Cm—Ca—Cb	126.0	125.7	125.4	122.8(3)	130.4(3)
Ca—Cb—CH _x		125.3		123.6(3)	132.5(4)
Cb—Cb—CH _x		127.8		127.9(3)	121.2(4)

^a From the least-squares plane of the 24 core atoms, except for H₂DAP which uses the least-squares plane of the nitrogen atoms. ^b Estimated errors (from ref 1): H₂P, 0.004–0.007 \AA ; H₂OEP, 0.002 \AA ; H₂TPrP, 0.004 \AA . ^c Estimated errors (from ref 1): H₂P, 0.3–0.5°; H₂OEP, 0.1°; H₂TPrP, 0.2–0.4°.

positions are seen for the N—Ca—Cm, Ca—Cm—Ca, Cm—Ca—Cb, Ca—Cb—CH_x, and Cb—Cb—CH_x bond angles. These differences are far larger than those expected for simple substituent effects, e.g. H₂OEP or H₂TPrP versus porphyrin 10 (Table 4). However, the differences are consistent with the macrocycle conformation minimizing repulsions between the meso and pyrrole ethyl groups by moving them further apart. This is achieved by narrowing the Ca—Cm—Ca angle, decreasing the N—Ca—Cm angle (or increasing the Cm—Ca—Cb angle), and decreasing the Cb—Cb—CH_x angle (or increasing the Ca—Cb—CH_x angle). The fact that the average values for the N—Ca—Cm, Ca—Cm—Ca, Cm—Ca—Cb, Ca—Cb—CH_x, and Cb—Cb—CH_x bond angles in H₂DAP are quite close to the average values in H₂OEP and H₂TPrP (Table 4) suggests that angle changes which decrease the steric crowding of the meso ethyl substituents are offset by opposing distortions at the unsubstituted meso positions; i.e., it appears that strain energy is being redistributed within the molecule.

The crystal structure of the corresponding nickel(II) complex (NiDAP) is shown in Figures 5 and 6. NiDAP is characterized by a large ruffling distortion¹⁵ of the porphyrin macrocycle, with the pyrrole rings being rotated on average by 23.8° against the

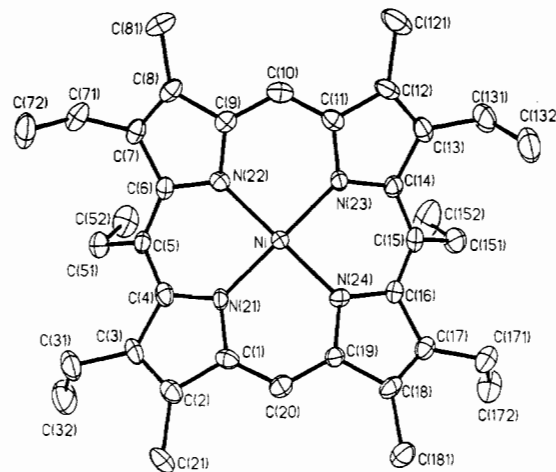


Figure 5. Molecular structure and numbering scheme for the crystal structure of NiDAP. Ellipsoids are drawn for 50% occupancy; hydrogen atoms have been omitted for clarity.

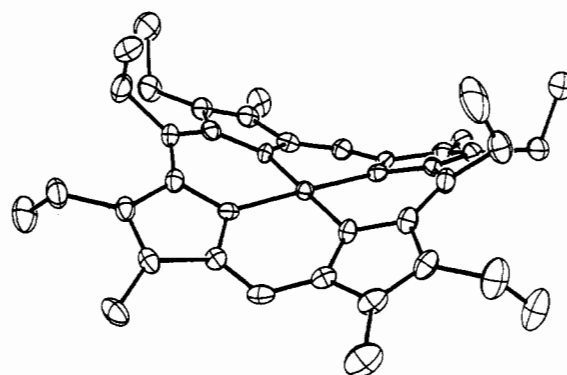


Figure 6. View of the macrocycle conformation in the crystal structure of NiDAP. Hydrogen atoms have been omitted for clarity.

least-squares plane of the nitrogen atoms. This gives rise to a roof structure similar to that seen for CuDAP¹⁷ and other metal complexes of decaalkylporphyrins.^{27,28} The macrocycle is essentially square ($N(21)-N(22)/N(23)-N(24) = 2.64 \text{ \AA}$, $N(21)-N(24)/N(22)-N(23) = 2.73 \text{ \AA}$), and the average Ni—N bond distance is quite short [$1.900(4) \text{ \AA}$]. Consistent with the nonplanar structure being an intrinsic feature of this porphyrin, there is also no evidence that the nonplanarity is a result of crystal packing forces. The conformation of NiDAP leads to a stacking pattern in which the roof edges point toward each other and the meso ethyl groups point in opposite directions. The molecules form layers with almost no overlap of the π systems, and a Ni—Ni separation of 7.60 \AA . The closest intermolecular contacts are 3.87 \AA for C(10)—C(7) and 3.67 \AA for C(12)—C(72).

Out-of-plane displacements for NiDAP are shown in Figure 7 and are summarized in Table 5. The mean deviation of the 24 porphyrin atoms from the least-squares plane of the nitrogen atoms is 0.37 \AA , with the difference between out-of-plane displacements for the substituted and unsubstituted meso positions being quite large. The meso carbons with ethyl substituents are displaced about 31% more than the unsubstituted meso positions. Such distortions of the substituted meso positions have been found in a number of nickel(II) porphyrins, and the concept of localized distortion has been investigated with regard to its biological relevance.^{6,29} The displacements of the meso carbon atoms in

(27) Collman, J. P.; Chong, A. O.; Jameson, G. B.; Oakley, R. T.; Rose, E.; Schmittou, E. R.; Ibers, J. A. *J. Am. Chem. Soc.* **1981**, *103*, 516.

(28) Lay, K.-K.; Buchler, J. W.; Kenney, J.; Scheidt, W. R. *Inorg. Chim. Acta* **1986**, *123*, 91.

(29) (a) Barkigia, K. M.; Thompson, M. A.; Fajer, J.; Pandey, R. K.; Smith, K. M.; Vicente, M. G. H. *New J. Chem.* **1992**, *16*, 599. (b) Senge, M. O.; Smith, N. W.; Smith, K. M. *Inorg. Chem.* **1993**, *32*, 1259.

Table 5. Average Out-of-Plane Displacements, Bond Lengths, and Bond Angles for NiDAP and CuDAP¹⁷ (Values in Parentheses from Minimum-Energy Structures Calculated Using the Force Field Described in the Experimental Section)

	NiDAP		CuDAP	
	meso H	meso ethyl	meso H	meso ethyl
Displacements (Å)^a				
M		0.02 (0.13)		0.04 (0.18)
N		0.01 (0.00)		0.00 (0.00)
Ca	0.40 (0.37)	0.47 (0.28)	0.38 (0.33)	0.30 (0.20)
Cb	0.27 (0.40)	0.31 (0.01)	0.32 (0.40)	0.11 (0.12)
Cm	0.68 (0.60)	0.89 (0.70)	0.61 (0.51)	0.63 (0.57)
Bond Lengths (Å)				
M—N		1.900(4) (1.919)		1.975(2) (1.981)
N—Ca	1.372(9) (1.377)	1.383(7) (1.390)	1.371(3) (1.376)	1.382(3) (1.388)
Ca—Cb	1.444(8) (1.438)	1.460(10) (1.463)	1.441(3) (1.439)	1.463(3) (1.464)
Ca—Cm	1.379(8) (1.366)	1.394(9) (1.389)	1.381(3) (1.372)	1.407(3) (1.394)
Cb—Cb		1.351(9) (1.345)		1.352(3) (1.347)
Cb—CH _x	1.504(11) (1.484)	1.511(9) (1.493)	1.499(4) (1.484)	1.512(3) (1.493)
Cm—CH ₂		1.528(8) (1.498)		1.521(3) (1.499)
Bond Angles (deg)				
N—M—N adj	91.9(2) (92.4)	88.3(1) (87.1)	92.3(1) (92.4)	87.6(1) (86.5)
N—M—N opp		178.9(2) (173.4)		177.7(1) (169.6)
M—N—Ca	125.9(4) (125.5)	127.6(4) (128.8)	124.2(1) (124.8)	128.9(2) (128.4)
N—Ca—Cm	124.5(6) (125.5)	123.0(6) (122.8)	124.8(2) (126.1)	123.1(2) (123.3)
N—Ca—Cb	110.0(5) (110.5)	109.4(5) (109.1)	110.0(2) (109.8)	108.9(2) (108.4)
Ca—N—Ca		106.3(5) (105.7)		106.8(2) (106.8)
Ca—Cm—Ca	123.2(6) (123.7)	120.3(5) (118.4)	126.4(2) (125.4)	122.3(2) (119.8)
Ca—Cb—Cb	107.5(6) (107.4)	106.6(5) (107.1)	107.4(2) (107.6)	106.8(2) (107.3)
Cm—Ca—Cb	124.7(6) (123.9)	127.3(5) (128.0)	125.1(2) (124.1)	127.7(2) (128.3)
Ca—Cb—CH _x	124.0(6) (126.1)	128.4(6) (128.4)	124.0(2) (126.1)	130.5(2) (128.3)
Cb—Cb—CH _x	128.5(6) (126.5)	124.4(6) (124.4)	128.6(2) (126.4)	122.2(2) (124.2)

^a From the least-squares plane of the nitrogen atoms.

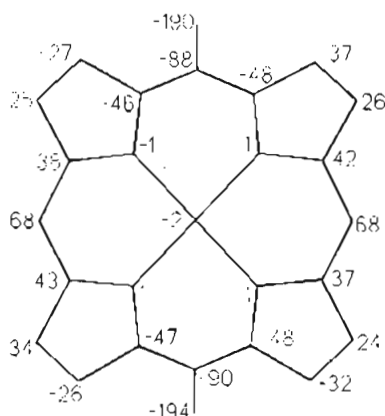


Figure 7. Deviations of atoms from the least-squares planes of the four nitrogen atoms in the crystal structure of NiDAP (Å × 10²).

NiDAP are larger than those observed in CuDAP,¹⁷ which is consistent with the known tendency of smaller metal ions to favor a more nonplanar structure.^{1,2,12}

The bond lengths and bond angles for NiDAP and CuDAP¹⁷ are summarized in Table 5. Interestingly, the differences in the N—Ca—Cm, Ca—Cm—Ca, Cm—Ca—Cb, Ca—Cb—CH_x, and Cb—Cb—CH_x bond angles seen for the substituted and unsubstituted meso positions of NiDAP and CuDAP are qualitatively similar to those seen for H₂DAP, although in absolute terms the differences are smaller for the metalloporphyrins. The steric repulsions in H₂DAP and NiDAP seem to be minimized to about the same degree, as judged by the distances between the methylene carbons of the pyrrole and meso ethyls (NiDAP, 3.16 ± 0.01 Å; H₂DAP, 3.13–3.23 Å) and the distances between the meso methylene carbons and Cb atoms (NiDAP, 3.13 ± 0.1 Å; H₂DAP, 3.09–3.12 Å). In a general sense, it appears that in NiDAP the strain between the substituents is relieved by a nonplanar distortion of the macrocycle, whereas in H₂DAP steric strain is relieved by bond angle changes. As several porphyrins (e.g. NiOEP²⁴) are known to crystallize in both planar and nonplanar conformations,^{1,2} it is interesting to speculate whether the steric

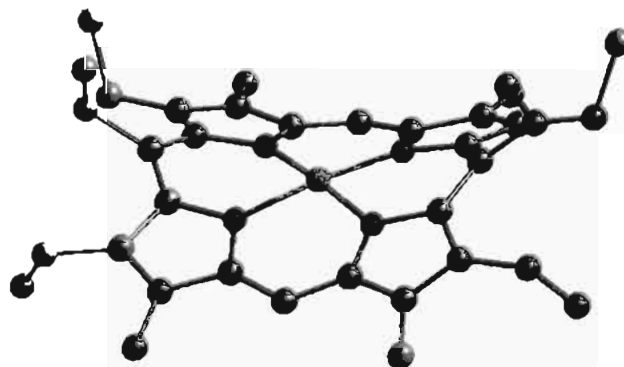


Figure 8. Minimum-energy structure calculated for NiDAP using the force field described in the Experimental Section. The ethyl orientations were taken from the crystal structure of NiDAP (Figure 6).

crowding in H₂DAP can also be minimized by the molecule adopting a nonplanar conformation.

Molecular Mechanics Calculations. The conformations of NiDAP and CuDAP were investigated by molecular mechanics calculations, using the force field described in the Experimental Section. Initially, planar porphyrins with the same ethyl orientations seen in the crystal structures of NiDAP and CuDAP were constructed and energy-minimized. These structures were then subjected to molecular dynamics simulations and re-minimized, with this process being repeated until no change in the calculated structure was noted. The conformations of these minimum-energy structures were found to be similar to those determined crystallographically, as evidenced by a comparison of the calculated structure of NiDAP (Figure 8) with the crystal structure (Figure 6). Average bond lengths, bond angles, and out-of-plane displacements calculated for NiDAP and CuDAP are recorded in Table 5, alongside those measured for the corresponding crystal structures. The calculations generally reproduce the bond lengths and bond angles, as well as the differences in bond angles for substituted and unsubstituted positions, with a high degree of accuracy. As noted previously,^{11,13} the calculations tend to slightly underestimate the Cb—CH_x and Cm—CH_x bond lengths. The agreement between the observed

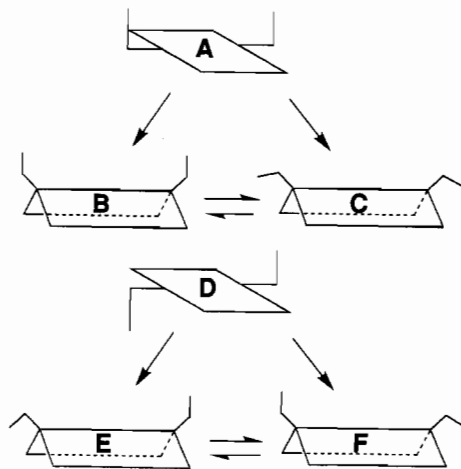


Figure 9. Representations of the structures and conformational equilibria proposed for the DAP molecule in solution.

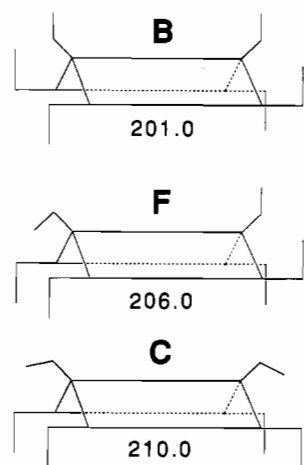


Figure 10. Structures and relative energies ($\text{kcal}\cdot\text{mol}^{-1}$) calculated for diaxial (B), trans (F), and diequatorial (C) conformers of ZnDAP using the force field described in the Experimental Section. The orientations of the pyrrole ethyl groups are those which give the lowest calculated energies.

and calculated out-of-plane displacements is reasonable for both CuDAP and NiDAP. The rms errors obtained when the crystal and calculated structures are matched are 0.15 Å for NiDAP and 0.10 Å for CuDAP. The rms error for NiDAP is significantly larger than the errors typically measured for very nonplanar dodeca-substituted porphyrins (0.07–0.11 Å),^{11,12} although why this should be the case is not clear at present.

To address the question of the two conformations observed in solution for ZnDAP,¹⁶ extensive molecular modeling studies were carried out. The relative orientations of the pyrrole and meso ethyl groups were systematically varied for both planar and ruffled macrocycles prior to energy minimization. The relative orientations of the pyrrole and meso ethyl groups were also changed after minimization, and the structures reminimized. Some structures were also subjected to molecular dynamics simulations and then reminimized. The global-minimum-energy conformation obtained for ZnDAP was a roof structure in which the meso ethyl groups adopted axial conformations (structure B in Figure 9). The pyrrole ethyl groups had the methyl groups pointing alternately up and down (structure B in Figure 10). The axial meso ethyls were also slightly twisted so that the methyls of the meso ethyls were above the down methyls of the pyrrole ethyls. This structure is quite similar to the crystal structures of NiDAP and CuDAP,¹⁷ except for the orientations of the pyrrole ethyl groups, which are different in all three structures. On this point it should be noted that the molecular mechanics calculations show that several structures with different conformations of the pyrrole

Table 6. Absorption Maxima (nm) for Free-Base Porphyrins and Nickel(II) and Zinc(II) Complexes in Dichloromethane

H ₂ TPP	414	514	548	588	646
H ₂ DAP	410	512	546	582	632
H ₂ OETPP	456	546	592	630	694
NiTPP	414	525	557		
NiDAP	418	548	578/596		
NiOETPP	433	552	585		
ZnTPP ^a	428	562 ^b			
ZnDAP ^a	428	562 ^b			
ZnOETPP ^a	468	610	660		

^a In dichloromethane plus pyridine. ^b The usual two-band pattern is not seen, so the most intense band is given.

ethyl groups but basically the same roof structure of the macrocycle are less than 2 $\text{kcal}\cdot\text{mol}^{-1}$ higher in energy than the global-minimum-energy structure for ZnDAP. This suggests that the orientations of the pyrrole ethyl groups observed in the crystal structures could easily be the result of crystal packing forces. The calculated displacements for ZnDAP show that it is more planar than CuDAP and much more planar than NiDAP. This agrees with previous observations that larger metal ions tend to favor more planar macrocycle conformations.^{1,2,12}

The diaxial structure is only one member of a family of syn structures. If one of the meso ethyls is switched to an equatorial position, this generates a trans arrangement of the methyl groups of the meso ethyls (structures E and F in Figure 9). The minimum-energy structure for this arrangement of the meso ethyl groups retains a roof conformation of the macrocycle but is 5.0 $\text{kcal}\cdot\text{mol}^{-1}$ higher in energy than the diaxial conformation (Figure 10). Switching both ethyl groups to equatorial positions (structure C in Figure 9) gives a roof structure which is calculated to be 9.0 $\text{kcal}\cdot\text{mol}^{-1}$ higher in energy than the diaxial conformation (Figure 10). Note that in both trans and diequatorial conformations the orientations of the pyrrole ethyl groups were optimized to give the lowest energy structures, and that in each case several other conformations of the pyrrole ethyl groups were found which were less than 2 $\text{kcal}\cdot\text{mol}^{-1}$ higher in energy. A conformational search was also made for anti conformations of ZnDAP.¹⁶ Structures similar to the anti conformation shown in Figure 2 were seen as local energy minima. The lowest energy anti conformation was calculated to be 7.4 $\text{kcal}\cdot\text{mol}^{-1}$ higher in energy than the global-minimum-energy structure (B in Figure 10) and therefore 2.4 $\text{kcal}\cdot\text{mol}^{-1}$ higher in energy than the trans structure (F in Figure 10). This suggests that an anti structure is not the second species observed in low-temperature NMR studies of ZnDAP.¹⁶ In support of this suggestion, none of the crystal structures reported for 2,3,5,7,8,12,13,15,17,18-decaalkylporphyrins^{17,27,28} show anti conformations. Interestingly, a trans conformation similar to structure F in Figure 10 is seen in the crystal structure of two porphyrins linked at the 5,15 positions by six atom chains to form a dimer.²⁷

Optical Spectroscopy. Several studies have shown that nonplanar conformational distortions in porphyrins cause shifts in the optical spectra to absorption at lower energy.^{7–11,13,14} This potentially provides a simple test of whether the conformations of H₂DAP and NiDAP in solution are similar those seen in the crystal structures. Absorption maxima measured from the optical spectra of H₂DAP, ZnDAP, and NiDAP are given in Table 6, together with absorption maxima for H₂TPP (8) and the very nonplanar porphyrin H₂OETPP (1). The absorption maxima for H₂DAP are similar to those for H₂TPP, implying that H₂DAP is planar or nearly planar in solution. The conformation of H₂DAP in solution therefore seems similar to that determined crystallographically. The absorption maxima for NiDAP are red-shifted compared to those for NiTPP and, in some cases, are close to the absorption maxima for NiOETPP. This suggests the NiDAP adopts a very nonplanar conformation in solution, which is also consistent with the crystallographic data for this porphyrin.

Table 7. Proton NMR Data for H₂DAP, ZnDAP, and NiDAP in CD₂Cl₂^a

proton	H ₂ DAP ^b		ZnDAP ^c		NiDAP	
	293K	233K	293K	243K	293K	193K
meso H	10.08 (s) ^d	10.13 (s) ^e 10.00 (s)	9.91 (s)	9.89 (s) ^e 9.99 (s)	9.07 (s)	9.05 (s)
meso CH ₃ CH ₂	5.02 (q)	4.97 (m)	5.06 (q)	5.02 (m)	4.36 (q)	4.24 (q)
meso CH ₃ CH ₂	1.79 (t)	1.92 (t) 1.81 (t)	1.30 (br)	1.26 (t) ^e 1.73 (t)	0.67 (t)	0.58 (t)
pyrrole CH ₃	3.61 (s)	3.61 (s) 3.60 (s) ^e	3.54 (s)	3.51 (s) ^e 3.56 (s)	3.20 (s)	3.14 (s)
pyrrole CH ₃ CH ₂	4.02 (br)	4.04 (m) ^f 3.92 (m) ^f	4.03 (q)	4.00 (m)	3.74 (q)	3.65 (m) ^f
pyrrole CH ₃ CH ₂	1.79 (t)	1.77 (t) 1.75 (t)	1.83 (t)	1.82 (t) ^e 1.77 (t)	1.72 (t)	1.64 (t)
NH	-1.78 (s)	-1.98 (s)				

^a Chemical shifts are given in ppm and referenced to CHDCl₂ at 5.30 ppm. ^b $K = 1.14$ (lit.¹⁶ 1.2); $\Delta G_{233} = 0.1$ kcal·mol⁻¹ (lit.¹⁶ 0.1 kcal·mol⁻¹); $\Delta G_{273}^* = 14.3$ kcal·mol⁻¹ (lit.¹⁶ 14.2 kcal·mol⁻¹). ^c $K = 2.8$ (lit.¹⁶ 3.3); $\Delta G_{243} = 0.5$ kcal·mol⁻¹ (lit.¹⁶ $\Delta G_{233} = 0.6$ kcal·mol⁻¹); $\Delta G_{273}^* = 13.6$ kcal·mol⁻¹ (lit.¹⁶ 13.3 kcal·mol⁻¹). ^d s = singlet, t = triplet, q = quartet, m = multiplet, br = broad. ^e Signals for major (cis) component. ^f Diastereotopic methylene protons.

The optical spectrum of ZnDAP solvated with pyridine is similar to that seen for ZnTPP, indicating a planar or slightly nonplanar macrocycle. This is in reasonable agreement with the molecular mechanics calculations, which show a moderately nonplanar conformation.

Variable-Temperature Proton NMR Spectroscopy. Chemical shift assignments, equilibrium constants, free energy differences (ΔG), and free energies of activation (ΔG^*) obtained from variable-temperature NMR studies of H₂DAP, ZnDAP, and NiDAP are summarized in Table 7. The data for H₂DAP and ZnDAP are essentially identical with those reported previously¹⁶ and clearly show the presence of two species at low temperatures. Complexes with metals other than zinc(II) have not previously been investigated.¹⁶ In the present study, we also examined NiDAP using variable-temperature proton NMR spectroscopy and detected only one set of signals at low temperatures (Table 7).

On the basis of the energies calculated for different conformations of ZnDAP, it is reasonable to suppose that the two species seen in solution correspond to cis (diaxial) roof structures with different conformations of the pyrrole ethyl groups. Unfortunately, this model had to be rejected because it did not explain the ratios and chemical shifts of the two components. However, a model involving cis (diaxial) and trans orientations of the methyl groups of the meso ethyls could be used to rationalize the NMR data for ZnDAP, NiDAP, and H₂DAP. In this model, a planar porphyrin macrocycle (e.g. H₂DAP) exists as a mixture of structure A (the cis conformer) and structure D (the trans conformer) (Figure 9). When the molecule adopts a nonplanar roof structure (e.g. ZnDAP), the meso ethyl groups can be in one of two positions designated axial and equatorial. This gives four possible conformations: diaxial (B), diequatorial (C), and two equivalent trans conformations (E and F) (Figure 9).

It was assumed that the two species observed in solution for ZnDAP would be the diaxial and trans conformations, because these have the lowest calculated energies. In this case, a total of three signals is expected for the meso ethyl groups: one axial ethyl from the diaxial conformation and one axial and one equatorial ethyl from the trans conformation. In fact, only two meso ethyl signals are observed experimentally. The model therefore requires some mechanism for interconverting the axial and equatorial ethyl groups of the trans conformation to give only one signal. This interconversion could be accomplished by macrocyclic inversion, a process which is frequently observed for dodecasubstituted porphyrins.^{7-9,11,13} It is reasonable to assume that a similar effect occurs for metal complexes of DAP, especially as macrocyclic inversion was recently observed for the nickel(II) complex of porphyrin **11** (Ni**11**).¹¹ Ni**11** has alkyl substituents at the pyrrole and meso positions and is therefore structurally related to NiDAP. It also adopts a nonplanar conformation which

is similar to that observed for NiDAP, although in the case of Ni**11** the alkyl substituents are found in both axial and equatorial positions in the crystalline state.¹¹ At room temperature the proton spectrum of Ni**11** shows a single set of signals for each group of protons in the molecule. However, upon cooling, the meso ethyls split into several signals of differing intensity, corresponding to conformations with various combinations of axial and equatorial ethyl groups. More importantly, the number of signals observed for the meso ethyls indicates another process which is fast on the NMR time scale. This process, presumably macrocyclic inversion, interconverts axial and equatorial positions of the ethyl groups while retaining their relative orientations. A similar process could provide the averaging of the axial and equatorial environments required in the present case.

Predictions based on the cis-trans model were then compared with the experimental data. The solution conformation of H₂DAP was considered first. On the basis of the crystal structure and optical data for H₂DAP, it is reasonable to assume that this porphyrin is planar or nearly planar in solution. Cis and trans arrangements of the methyl of the meso ethyl groups (A and D in Figure 9) are thus expected to have similar energies. On this basis, the cis-trans model predicts an equilibrium constant close to 1; the observed value of 1.14 is in excellent agreement with this prediction. The effect of the structure on the proton chemical shifts was also analyzed. Protons in the cis and trans forms of a planar or nearly planar macrocycle are expected to have similar geometric relationships to the porphyrin macrocycle, so they should also have similar chemical shifts. The chemical shifts for H₂DAP given in Table 7 also agree with this prediction.

For ZnDAP, the molecular mechanics calculations and optical data are consistent with a moderately nonplanar roof conformation. The molecular mechanics calculations also indicate that the diaxial conformation should predominate over the trans conformation (Figure 10), so the equilibrium constant should be larger for ZnDAP than for H₂DAP. In agreement with this prediction, the observed equilibrium constant is 2.8. Specific predictions could also be made about the proton chemical shifts of the two components seen at low temperatures for ZnDAP. These predictions are based on the observation that the porphyrin ring current effect will shift the methyl signal of an axial meso ethyl upfield in comparison to the methyl signal of an equatorial meso ethyl.¹¹ The methyl signal of the diaxial conformation is therefore expected to shift to higher field compared to that of the trans conformation. The chemical shifts of the remaining protons in the molecule should be relatively unaffected because they are expected to keep essentially the same geometric relationship with the porphyrin macrocycle. In agreement with these predictions, the methyl signal of the major component, assigned as the diaxial conformation, is found at 1.26 ppm and the methyl signal of the minor component is found at 1.73 ppm. Furthermore, the

chemical shifts of the remaining protons are quite similar in both components (Table 7). Finally, it should be noted that the observed energy difference between the two species ($\Delta G_{243} = 0.5$ kcal·mol⁻¹) is much smaller than the calculated energy difference between the diaxial and trans conformations of ZnDAP (5.0 kcal·mol⁻¹). This could occur because the force field used in the calculations is quite general in nature or because solvation effects were not considered. In either case, the qualitative agreement between the observed and calculated conformational energies lends further support to the use of molecular mechanics calculations in studies of this kind.

The cis–trans model can also be used to make predictions about the kinetics of the dynamic processes observed for ZnDAP and H₂DAP.¹⁶ If the process seen for ZnDAP and H₂DAP is simply ethyl rotation, it is reasonable to assume that a more nonplanar structure will move the meso ethyl groups further out of plane. This would presumably lower the energy barrier for ethyl rotation and hence increase the interconversion rate as nonplanarity increases, i.e. in the series H₂DAP < ZnDAP < NiDAP. Consistent with this prediction, the reported¹⁶ interconversion rate for ZnDAP (850 s⁻¹ at 296 K) is higher than the rate measured for H₂DAP (180 s⁻¹ at 296 K).

Finally, the cis–trans model was applied to NiDAP, which showed only one set of proton NMR signals at low temperatures. The crystallographic data, molecular mechanics calculations, and optical studies all suggest that NiDAP adopts a highly nonplanar roof structure. Molecular mechanics calculations also indicate that the difference in energy between the diaxial and trans conformations is larger for the more nonplanar NiDAP molecule than for ZnDAP, so the diaxial conformation should be even more dominant in solution for NiDAP. If the population of the trans conformation is too small to detect, this could explain why only one set of signals is seen at low temperatures. However, the cis–trans model also predicts that the very nonplanar conformation of NiDAP will lower the barrier for ethyl rotation and increase the interconversion rate. If interconversion between the diaxial and trans forms was rapid on the NMR time scale even at the lowest temperatures studied, this could also explain why only one set of signals is observed.

The NMR data for NiDAP (Table 7) shed some light on this matter. The chemical shift of the methyl protons of the meso ethyl groups in NiDAP (0.67 ppm) is similar to the range of values measured for axial ethyl groups in Ni11 (0.80–0.89 ppm), whereas the methyl protons of an equatorial ethyl group in Ni11 resonate at 2.22 ppm.¹¹ This suggests that the diaxial conformation of NiDAP is highly favored in solution but does not preclude the possibility that ethyl rotation is also rapid on the NMR time scale.

Conclusions

The crystal structure of 3,5,7,13,15,17-hexaethyl-2,8,12,18-tetramethylporphyrin (H₂DAP) reveals an essentially planar macrocycle which is unusually elongated along the 5,15 axis in order to relieve the steric crowding of the meso and pyrrole ethyl groups. This structure is particularly interesting because crowding of the substituents in highly substituted porphyrins is normally relieved by nonplanar distortions of the porphyrin macrocycle,^{9,11,12,14,17} as typified by the crystal structure of (3,5,7,13,15,17-hexaethyl-2,8,12,18-tetramethylporphyrinato)nickel(II) (NiDAP), which is also reported here.

The crystal structures of NiDAP and CuDAP¹⁷ can be predicted fairly accurately using a published molecular mechanics force field.^{10,12} The same force field was also used to investigate the solution conformations of the zinc(II) complex (ZnDAP). It has previously been proposed that the two species observed for ZnDAP, as well as H₂DAP, in low-temperature proton NMR studies arise from syn and anti conformations of the porphyrin macrocycle.¹⁶ In this work, we find that the available structural and spectroscopic data for ZnDAP, H₂DAP, and NiDAP are more consistent with the two species corresponding to cis and trans arrangements of the methyl groups of the meso ethyls.

The results presented here raise two interesting questions. First, do 2,3,5,7,8,12,13,15,17,18-decasybstituted free-base porphyrins always adopt a planar conformation similar to that seen for H₂DAP? Second, how do the 5,15 substituents influence the conformations of decasybstituted porphyrins? These and other questions will be addressed in a forthcoming publication.³⁰

Acknowledgment. This work was supported by grants from the National Science Foundation (K.M.S., CHE-93-05577), the National Institutes of Health (K.M.S., HL-22252), the Deutsche Forschungsgemeinschaft (M.O.S.), and the U.S. Department of Energy (J.A.S., DE-ACO4-76DPOO789). C.J.M. and J.D.H. thank the Associated Western Universities, Inc., for Postdoctoral Fellowships. The assistance of Karen Fruhbauer in the preparation of the manuscript is gratefully acknowledged.

Supplementary Material Available: Tables of bond lengths, bond angles, anisotropic displacement coefficients, and hydrogen atom coordinates and isotropic displacement coefficients for H₂DAP (6) and NiDAP (Ni6) (7 pages). Ordering information is given on any current masthead page.

(30) Senge, M. O.; Medforth, C. J.; Forsyth, T. P.; Hobbs, J. D.; Pandey, R. K.; Olmstead, M. M.; Shelnut, J. A.; Smith, K. M. Manuscript in preparation.